Distributed Acoustic Sensing for detecting near surface hydroacoustic signals

Alexander S. Douglass[1], Alexander S Douglass[2], Shima Abadi[2], and Bradley P Lipovsky[3]

[1]Affiliation not available
[2]School of Oceanography, University of Washington
[3]Department of Earth and Space Sciences, University of Washington

March 16, 2023

Distributed Acoustic Sensing for detecting near surface hydroacoustic signals

Alexander S. Douglass,[1,a] Shima Abadi,[1] and Bradley P. Lipovsky[2]

[1] *School of Oceanography, University of Washington, Seattle, WA 98195, USA; asd21@uw.edu, abadi@uw.edu*

[2] *Department of Earth and Space Sciences, University of Washington, Seattle, WA 98195, USA; bpl7@uw.edu*

Abstract

Distributed Acoustic Sensing (DAS) is a technology in which a fiber-optic cable is turned into an acoustic sensor by measuring backscatter of light caused by changes in strain from the surrounding acoustic field. In October 2022, 9 days of DAS and co-located hydrophone data were collected in Puget Sound near Seattle, WA. Passive data was continuously recorded for the duration and a broadband source was fired from several locations and depths on the first and last days. This dataset provides direct comparisons between DAS and hydrophone measurements, and demonstrates the ability of DAS to measure acoustics signals up to ~500Hz.

Keywords: Distributed Acoustic Sensing, Submarine Fiber Optic Cable

[a] Author to whom correspondence should be addressed.

1. Introduction

Acoustic monitoring is an important component of studying the wide variety of sounds and sound sources in the ocean. Applications of ocean acoustics range from general oceanography, studying of marine mammals, monitoring of natural and anthropogenic ocean noise, defense, ocean exploration, and more. Unfortunately, dense sampling of the acoustic field in large regions of the ocean can be impractical. Deployment of large hydrophone arrays is challenging - the hydrophones may be expensive and often require maintenance (which is particularly challenging for deeper regions of the ocean), and denser sampling is only achieved by deploying more hydrophones. Thus, alternatives that allow for increased coverage of the ocean at reduced cost are highly desirable.

Distributed fiber optic sensing (DFOS) is a class of techniques in which a fiber-optic cable, typically used for data transfer, acts as the sensor, capable of measuring temperature (Distributed Temperature Sensing, DTS), strain (Distributed Strain Sensing, DSS), or vibrations (Distributed Acoustic Sensing, DAS) (Bao and Chen 2012). The use of fiber optic cables to measure acoustic waves (DAS) is a recent development in this class of measurement techniques. DAS utilizes Rayleigh backscattering of light from nano-scale defects in the fibers to measure acoustic waves (Hartog, 2017; Masoudi and Newson 2015). An interrogator device attached to one end of the cable sends repeated laser pulses through the cable and as these waves interact with the fibers, phase changes in the scattered light over small sections of cable (the gauge length) allow spatially resolved measurement of strain or strain-rate. These strain and strain-rate measurements provide information about the average acoustic field over the chosen gauge length, sampled at regular intervals along the cable. The gauge length and sampling resolution are both parameters that can be varied depending on the application and limitations of the cable. The ranges over which the cables can be used to sense the acoustic field can be limited by several factors: the distance to the first repeater (if applicable), the attenuation along the fiber resulting in an SNR that is too low, or the sampling rate (such that each light pulse has enough time to travel to the desired point along the cable, and the backscattered light to propagate back to the interrogator, prior to the next pulse). Frequency capabilities are still an active area of exploration, but are known to extend to at least several hundred Hz (Taweesintananon et al. 2021, Lindsey and Martin 2021).

DAS was first explored as a technique for seismic applications and has received significant attention in that community over the last decade. The first demonstration of DAS was in 2009, using the technology as a replacement for borehole geophones, with additional similar field trials in 2010 (Mestayer et al. 2011). These initial field trials demonstrated the ability to do seismic imaging with DAS and produce comparable results to geophone-produced images in terms of signal-to-noise ratio and resolution. Additional demonstrations of DAS technology, capabilities, and applications followed over the next decade and it has become a significant area of research in seismology (Dou et al. 2017, Karrenbach et al 2018, Zhan et al. 2020, Lindsey et al. 2019, Sladen et al. 2019).

Recently, DAS has been explored as a means for measuring acoustic fields at frequencies above those typically relevant for seismic applications (>20 Hz). By extending DAS capabilities to higher frequencies, the technology can be utilized for measurements of acoustics in the water column. To date, only a small number of demonstrations of DAS for water column acoustics have been completed. DAS has shown the ability to produce seismic images comparable to those generated by a typical towed array method, particularly utilizing the lower spectral content of the seismic source and when the offset range did not exceed the channel depth (Taweesintananon et al. 2021, Matsumoto et al. 2021). Ship detection and tracking with signals up to 100 Hz has seen success in both shallow and deep water channels, with deeper water performing better due to lower SNRs (Rivet et al. 2021). Finally, additional ship tracking and detection of baleen whale calls below 100 Hz using a cable in the arctic (Bouffaut et al. 2022, Landrø et al. 2021) and ship noise and fin whale calls (<20 Hz) utilizing a cable from the Ocean Observatories Initiative (Wilcock et al. 2023) have been demonstrated.

The focus of this manuscript is on an active-source experiment conducted in the Puget Sound near Seattle, WA. The goal for this data is two-fold - to explore the capabilities of DAS at frequencies up to 1 kHz, and to provide hydrophone measurements taken close to the cable for direct comparison of the DAS measurements. The remainder of this manuscript provides a detailed overview of the experiment and a brief overview of some of the DAS measurements.

2. DASCAL22 Experiment

The DAS Calibration 2022 (DASCAL22) experiment took place in the Saratoga Passage region of the Puget Sound in Washington State from October 19th, 2022 to October 28th, 2022. In this experiment, three hydrophones were deployed adjacent to a fiber-optic DAS cable is buried in the seabed between Camano Island and Whidbey Island. The water depth varies from 0 m (at the entry points to the water), to a maximum of ~100 m, with the majority of the cable lying between ~80-90 m depth. The approximate location of the cable and the bathymetry along the cable are shown in Figs 1a and 1b, respectively. A mooring with three hydrophones was deployed next to the cable at ~93 m depth. Two hydrophones, a SQ26-H1B and a CR1A (hydrophones A and B, respectively), were moored roughly 5 m from the sea floor, and a third hydrophone, another CR1A (hydrophone C), was moored roughly 25 m from the sea floor (all hydrophones provided by Cetacean Research Technology, Seattle, WA). The mooring location and layout are shown in Figures 1b and 1c, respectively. The hydrophones all recorded ~9 days of passive acoustic data with 44.1 kHz sampling rates. During the mooring deployment and recovery days, an acoustic source providing broadband impulsive signals was broadcast from three different depths (1 m, 5 m, and 10 m) at 5 second intervals from various locations near the mooring (with the boat's engine turned off during these broadcasts). The results shown in this paper are from the data recorded on the recovery day (28 October, 2022) when the current was weak, leading to a smaller variation in position during the broadcasts.

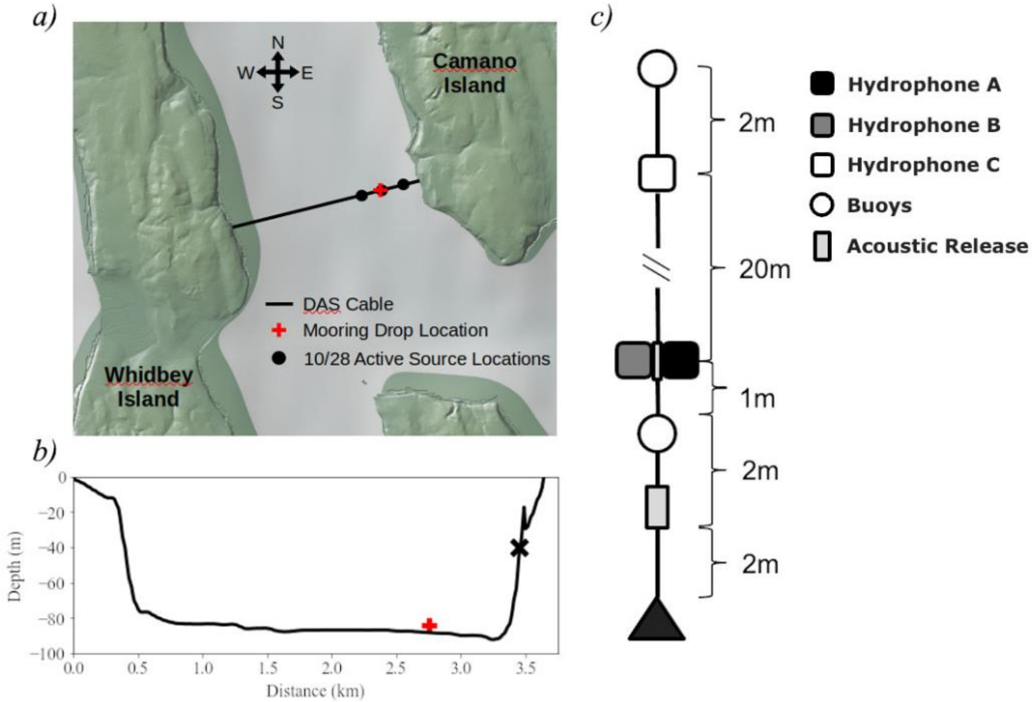

Fig. 1. DASCAL22 experimental setup. (a) The locations of the DAS cable, mooring, and active source testing, (b) the bathymetry along the DAS cable with the mooring location indicated by a red '+' and approximate location of the DAS channels considered in this study indicated by a black 'x'. (c) The mooring layout.

The acoustic source used during the experiment was a bubble pulser designed for geophysical surveys. The source consists of two electromechanical plates that are drawn together by applying a voltage to the plates, reversing direction after impacting, thus producing short-duration impulsive signals. In all broadcasts, the endfire dimension (along the face of the plates) was aligned parallel to the boat. On the equipment deployment day (19 Oct), a small reference hydrophone, an HTI-96-Min (High Tech, Inc., Long Beach, MS), was mounted 1 m from the center of the source to measure the signature from both broadside and endfire orientations at a 2 kHz sampling rate, allowing for characterization of the source signal measured by the moored hydrophones and DAS cable. Figure 2a provides a normalized spectral average of 10 shots (per curve) at 5 m depth, at both endfire and broadside orientations, as well as an ambient noise curve for reference, taken using windows of data just prior to the shot recordings. A 15 Hz high pass filter is applied to all data, as well as a 1 Hz bandpass filter at 60, 180, 300, 420, 540, 660, 780, and 900 Hz, compensating for amplitude spikes caused by equipment noise at multiples of 60 Hz (this compensation is imperfect, and as a result, some sharp amplitude fluctuations are still visible at some of these frequencies). These plots show that the source provides a broadband signal with significant SNR across most of the frequency spectrum. Most notably, a significant amount of acoustic energy exists between ~350-600 Hz in the endfire direction, and the broadside direction seems to provide a stronger signal at lower (<200 Hz) frequency ranges. Figure 2b shows a time domain measurement of three DAS channels (described next) with the source fired from three different depths and locations, demonstrating the capability of DAS to detect this source impulse. The Lloyd's mirror effect is noticeable in all three signals.

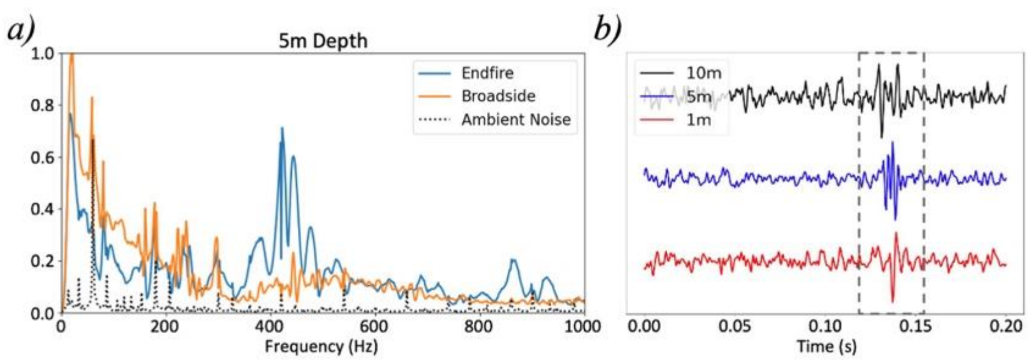

Fig. 2. (a) Spectra of the bubble pulser measured by a hydrophone mounted approximately 1 m from the source center at endfire (blue) and broadside (orange) while at a 5 m depth. (b) Time domain measurements of the bubble pulser

broadcasting from three depths (1, 5, and 10 m) at DAS channels 427, 431, and 433, respectively.

The submerged portion of the DAS cable is just over 3.5 km long, the full length of which was sampled at a 2 kHz sampling rate. A gauge length of 6.38 m and spatial resolution of 6.38 m were used. Though the water entry and exit points are known exactly, the precise positions on the seafloor are not perfectly known and are simply interpolated between these two points. DAS data was collected by Sintela Onyx v1.0 interrogator.

Over the 9 days between the equipment deployment and recovery, the three moored hydrophones and DAS cable generated ~4 TB of data and measured the acoustic field continuously, during which time there was significant boat traffic and a variety of weather, including windy and rainy conditions. The focus of this paper is only on the bubble pulser data recorded on the last day of deployment.

3. Results & Discussion

This data set provides an opportunity for direct comparison of DAS and hydrophone measurements, and can be used for calibrating DAS outputs for proper representation of ocean acoustic data. The goal for this manuscript, beyond the introduction of this experiment and dataset, is to demonstrate that DAS is capable of measuring an acoustic field at ranges >100 Hz. Figure 3 demonstrates one example of such a recording. Six consecutive shots from the active source, broadcast on the equipment recovery date (10/28), are plotted with data recorded by hydrophone A (Figure 3a), showing a clear broadband signal with notable SNR. The output of a single

DAS channel (channel 431) over the same period of time also clearly shows measurements of six pulses, with notably lower SNR, but still clearly visible between ~300-450 Hz (Figure 3b). The frequency response of a moving average with a period equal to the gauge length (6.38m) has frequency notches at ~235 Hz (speed of sound divided by gauge length) and ~470 Hz - notably the energy observed in these DAS signals are nicely within the bounds of these two notches. The Signal-to-Noise Ratio (SNR) for both hydrophone and DAS data is calculated from a 60 ms shot sample recorded at channel 431 and a 60 ms noise sample recorded 600 ms before the reception of the shot signal (Figure 3c). The SNR of the two measurements shows that the hydrophone measurements are significantly less noisy, but that significant improvements to the DAS SNR can are made by stacking 15 shots.

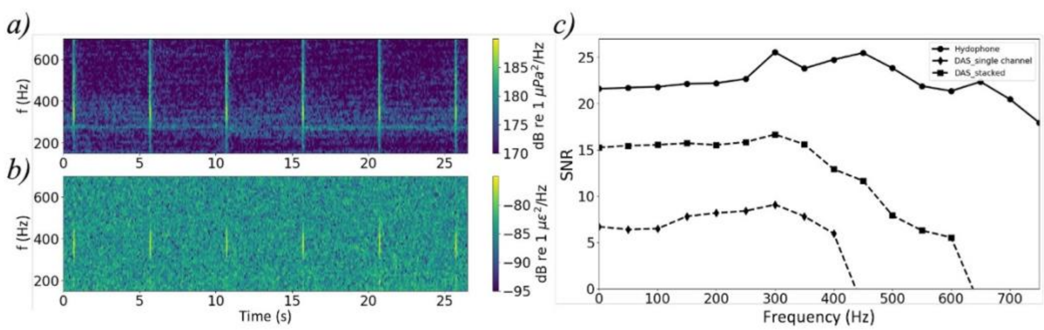

Fig. 3. (a) Six consecutive shots of the bubble pulser at 5 m below the surface measured by hydrophone A and (b) channel 431 of the DAS cable. (c) The SNR of the pulses as measured by hydrophone A, DAS channel 431, and DAS channel 431 with 15 shots stacked.

Figure 4 provides a waterfall plot of 200 consecutive time windows for two DAS channels (channel 427 in a, channel 431 in b) and hydrophone A (c), spanning ~20 minutes, at source depths of 10 m (shots 0-62), 5 m (shots 68-122), and 1 m (shots

128-186), with the source turned off during depth changes (evident in the waterfall plots), and the boat drifting with the current throughout the time window. During this time, the bathymetry at the source location varies from 66 m (starting) to 43 m (ending). The DAS measurements in both panels show a small time delay between two arrivals, corresponding to the direct path and surface reflection (note the delay shrinking when the source depth is decreased), as well as a slightly changing arrival time as the boat drifts further from the cable channels. The hydrophone shows similar characteristics, with time delayed surface reflections and a response slowly moving over time, as well as some multipath propagation. The first path corresponds to the direct path arrival, while the second is likely a path reflecting off of the sloped bathymetry, towards the hydrophone. The third path that arrives towards the top of the plot is likely due to a bathymetry change as the boat drifts, leading to a new, strong arrival. Note that the hydrophone is estimated to be ~750 m from the two DAS channels, thus the different impulse responses are expected. The two DAS channels shown here clearly pick up a direct path signal corresponding to the bubble pulser. The source is expected to be very close to these channels, thus a single strong arrival is expected. Additional arrivals, if they exist, may have lower SNRs that are undetectable, or propagate perpendicular to the cable where DAS has less sensitivity (Wilcock et al. 2023). Either of these may be the reason for a lack of signal detection in the first third of Figure 4b.

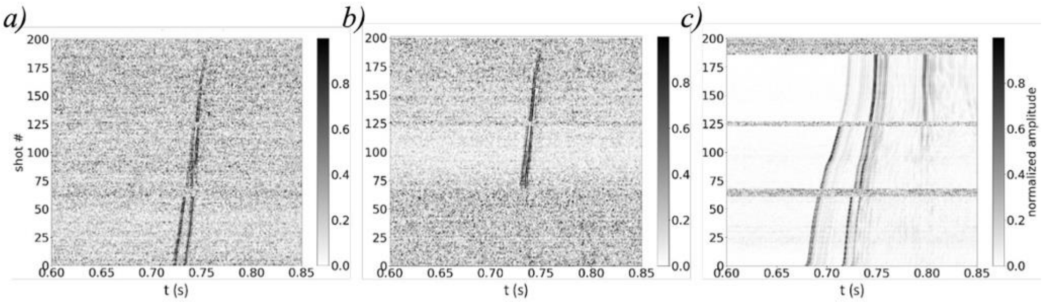

Fig. 4. Waterfall plots of ~200 shots of the bubble pulser for DAS channels (a) 427 and (b) 431 at , and for (c) hydrophone A. All plots begin at ~16:36:00 UTC.

These results demonstrate the ability of DAS to record acoustic signals at frequencies >100 Hz, up to nearly 500 Hz without stacking and up to nearly 700 Hz with stacking. Some of the limitations of DAS are also highlighted in these results: the inability to detect broadside signals and the low SNR achievable relative to hydrophones both may impact the measurements shown here. While the measurement taken by the hydrophones has clear advantages, the DAS cable provides some advantages as well - particularly in the sampling density. While the SNR in a DAS channel is significantly lower, the abundance of channels provides the capability to coherently combine measurements to increase SNR, on top of the advantages discussed previously. This data provides multiple opportunities to explore and improve the understanding of DAS capabilities in ocean acoustics, such as improving SNR, applying standard array signal processing techniques to the data, extension of measurements up to 1 kHz, and consideration of other acoustic sources available in these measurements.

4. Conclusions

DAS technology is an exciting frontier in ocean acoustics, potentially providing the ability to continuously monitor large regions of the ocean with dense arrays. However, the technology is in its infancy and significant work exists to fully exploit its capabilities. This experimental dataset provides a significant step towards this goal, with co-located hydrophone and DAS measurements, allowing for direct comparisons of the two measurements and calibration of signals recorded on DAS cables. An overview of the DASCAL22 experiment was provided and several conclusions from initial analysis of the data resulted.

First, it has been demonstrated that DAS technology is capable of detecting acoustic signals up to approximately 700 Hz, and it is likely that the capabilities extend to higher frequencies. Second, it is shown that the SNR of DAS cables is significantly lower than that of traditional hydrophone recordings, which was expected, but that some SNR can be recovered with clever combinations of measurements in the densely sampled array. In these results, a difference of ~5-15 dB SNR is seen, depending on whether the channels are stacked or single measurements. However the DAS channels used for this analysis are not co-located with the hydrophone, so this comparison is not direct. Third, we see evidence of the impact of arrival angle on DAS channel recordings, evidenced by the lack of multipath visible in DAS measurements shown here.

Acknowledgments

We thank the crew of the R/V Weelander in the School of Oceanography at the University of Washington. We also thank Dick Sylwester from the Northwest Geophysical Services for generously lending us his bubble pulser to use in our study.

References

Bao, X. and Chen, L. (**2012**). "Recent Progress in Distributed Fiber Optic Sensors," Sensors **12**, 8601-8639.

Bouffaut, L., Taweesintananon, K., Kriesell, H. J., Rørstadbotnen, R. A., Potter, J. R., Landrø, M., Johansen, S. E., Brenne, J. K., Haukanes, A., Schjelderup, O., and Storvik, F. (**2022**). "Eavesdropping at the Speed of Light: Distributed Acoustic Sensing of Baleen Whales in the Arctic," Front. Mar. Sci. **9**, 901348.

Daley, T. M., Freifeld, B. M., Ajo-Franklin, J., Dou, S., Pevzner, R., Shulakova, V., Kashikar, S., Miller, D. E., Goetz, J., Henninges, J., and Lueth, S. (**2013**). "Field testing of fiber-optic distributed acoustic sensing (DAS) for subsurface seismic monitoring," The Leading Edge **32**, 699-706.

Dou, S., Lindsey, N., Wagner, A. M., Daley, T. M., Freifeld, B., Robertson, M., Peterson, J., Ulrich, C., Martin, E. R., and Ajo-Franklin, J. B. (**2017**). "Distributed Acoustic Sensing for Seismic Monitoring of The Near Surface: A Traffic-Noise Interferometry Case Study," Sci. Rep. **7**, 11620.

Hartog, A. H. (2017). An introduction to Distributed Optical Fibre Sensors (CRC Press, Boca Raton, FL), p. 472.

Karrenbach, M., Cole, S., Ridge, A., Boone, K., Kahn, D., Rich, J., Silver, J., and Langton, D. (**2019**). "Fiber-optic distributed acoustic sensing of microseismicity, strain and temperature during hydraulic fracturing," Geophysics **84**, D11-D23.

Landrø, M., Bouffaut, L., Kriesell, H. J., Potter, J. R., Rørstadbotnen, R. A., Taweesintananon, K., Johansen, S. E., Brenne, J. K., Haukanes, A., Schjelderup, O., and Storvik, F. (**2022**). "Sensing whales, storms, ships and earthquakes using an Arctic fibre optic cable," Sci. Rep. 12, 19226.

Lindsey, N. J., Dawe, T. C., and Ajo-Franklin, J. B. (2019). "Illuminating seafloor faults and ocean dynamics with dark fiber distributed acoustic sensing," Science 366(6469), 1103–1107.

Lindsey, N. J., and Martin, E. R. (**2021**). "Fiber-optic seismology," Annu. Rev. Earth Planet. Sci. 49, 309–336.

Masoudi, A. and Newson, T. (**2016**). "Contributed Review: Distributed optical fibre dynamic strain sensing," Rev. Sci. Instrum. **87**, 011501.

Matsumoto, H., Araki, E., Kimura, T., Fujie, G., Shiraishi, K., Tonegawa, T., Obana, K., Arai, R., Kaiho, Y., Nakamura, Y., Yokobiki, T., Kodaira, S., Takahashi, N., Ellwood, R., Yartsev, V., and Karrenbach, M. (**2021**). "Detection of hydroacoustic signals on a fiber-optic submarine cable," Sci. Rep. **11**, 2797

Mestayer, J., Cox, B., Wills, P., Kiyaschenko, D., Lopez, J., Costello, M., Bourne, S., Ugueto, G., Lupton, R., Solano, G., Hill, D., and Lewis, A (**2011**). "Field Trials of Distributed Acoustic Sensing for Geophysical Monitoring," Society of Exploration Geophysicists, 4253-4257.

Rivet, D., de Cacqueray, B., Sladen, A., Roques, A., and Calbris, G. (**2021**). "Preliminary assessment of ship detection and trajectory evaluation using distributed acoustic sensing on an optical fiber telecom cable," J. Acoust. Soc. Am. **149**, 2615-2627.

Sladen, A., Rivet, D., Ampuero, J. P., De Barros, L., Hello, Y., Calbris, G., and Lamare, P. (2019). "Distributed sensing of earthquakes and ocean-solid Earth interactions on seafloor telecom cables," Nat. Commun. 10(1), 5777.

Taweesintananon, K., Landrø, M., Brenne, J. K., and Haukanes, A. (**2021**). "Distributed acoustic sensing for near-surface imaging using submarine telecommunication cable: A case study in the Trondheimsfjord, Norway," Geophysics **86**, B303-B320.

Wilcock, W. S. D., Abadi, S., and Lipovsky, B. (**2023**). "Distributed acoustic sensing recordings of low-frequency whale calls and ship noise offshore Central Oregon," JASA Express Lett. **3** (2).

Zhan, Z. (**2019**). "Distributed Acoustic Sensing Turns Fiber-Optic Cables into Sensitive Seismic Antennas," Seismol. Res. Lett. **91**, 1-15.